Supporting Information

for

Precision targeting of fat metabolism in triple negative breast cancer with biotinylated copolymer

By

Ruidas *et. al.*

Table of Contents

1. Materials and methods

Materials. 2, 2-dipyridyl disulfide (DPDS, 98%), 2-mercaptoethanol, dicyclohexylcabodiimide (DCC, 99%), 4-dimethylaminopyridine (DMAP, 99%), poly(ethylene glycol) methacrylate (HO-PEGMA, 500 g mol^{-1}), Biotin, 2,2'-azobis-(2-methylpropionitrile) (AIBN), and anhydrous *N*,*N*′-dimethylformamide (DMF, 99.9%), were purchased from Sigma-Aldrich and used without further purification, except for AIBN, which was used after recrystallization in methanol. Methacrylic acid was purchased from Merck Millipore India Pvt. Ltd. Polyethylene glycol methyl ether methacrylate (PEGMA, 300 g mol^{-1}, 99%) was purchased from Sigma-Aldrich and passed through a basic alumina column prior to polymerization. 1-Ethyl-3-(3-dimethylaminopropyl)carbodiimide was purchased from spectrochem Pvt. Ltd. The chain transfer agent (CTA), 4-cyano-(dodecylsulfanylthiocarbonyl)sulfanylpentanoic acid (CDP) was synthesized using literature procedure [1]. The NMR solvent, DMSO-d_6 (99% D) was purchased from Cambridge Isotope Laboratories, Inc., USA. The solvents such as dichloromethane (DCM), methanol (MeOH), hexanes (mixture of isomers), ethyl acetate were purified by following standard procedures.

Instrumentation. The ^{1}H NMR spectra were recorded on a JEOL-FT NMR-AL spectrometer operating at 400 MHz. Positive mode electrospray ionization mass spectrometry (ESI-MS) was performed on a Q-Tof Micro YA263 high resolution (Waters Corporation) mass spectrometer. Size exclusion chromatography (SEC) was used to obtain molecular weights and molecular weight distributions (dispersity, $Đ$) of polymers in THF solvent at 30 ^{o}C at a 1.0 mL/min flow rate. The instrument contains a Waters 515 HPLC pump, a Waters 2414 refractive index (RI) detector, one Polar Gel-M guard column (50 × 7.5 mm) and two Polar Gel-M analytical columns (300 × 7.5 mm). The UV–vis spectroscopic measurements were recorded on a Perkin–Elmer Lambda 35 spectrophotometer, with a scan rate of 120 nm/min.

Synthesis of 2-hydroxyethyl 2-pyridyl disulfide (PDS-OH): PDS-OH was synthesized following the literature procedure (Scheme S1) [2]. 2, 2'-dipyridyl disulfide (DPDS) (2.5 g, 11.3 mmol) was dissolved in 50 mL of methanol and 1 mL of glacial acetic acid was added as catalyst. To this mixture, a solution of 2-mercaptoethanol (0.44 g, 5.65 mmol) in 50 mL methanol was added dropwise at room temperature with continuous stirring. Once the addition was over, the reaction mixture was stirred at room temperature for an additional 3 h. The stirring was stopped, the solvent was removed by rotary evaporation. It was further purified by silica gel column chromatography using hexane/ethyl acetate as the mobile phase (4: 1 v/v) to get a colorless oil PDS-OH, with a yield of 70 %. ^{1}H NMR (Figure S1, DMSO-d_6, δ, ppm): 8.43 (m, 1H, aromatic proton ortho-N), 7.82 (m, 1H, aromatic proton meta-N), 7.80 (m, 1H, aromatic proton para-N), 7.23 (m, 1H, aromatic proton, ortho-disulfide linkage), 3.60 (t, 2H, -C***H***$_2$OH), 2.90 (t, 2H, -S-S-C***H***$_2$-).

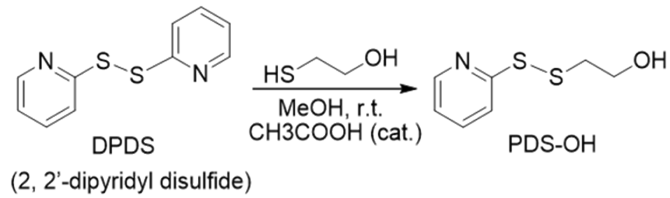

Scheme S1. Synthesis of PDS-OH.

Synthesis of 2-pyridyl disulfide methacrylate (PDSMA). The synthesis of vinyl monomer, PDSMA was performed by DCC/DMAP esterification [3] of methacrylic acid (MAA) and PDS-OH (Scheme S2). Briefly, MAA (1.03 gm, 12.02 mmol) was dissolved in 50 mL dry DCM, taken in a 100 mL round bottom flask and the solution was purged with dry N_2. Then, a solution of DCC (1.81 gm, 8.77 mmol) and DMAP (0.49 gm, 3.99 mmol) in 20 mL dry DCM was added to the solution, immersed in an ice-water bath with constant stirring. Then PDS-OH (1.5 gm, 8.01 mmol) was dissolved in 10 mL dry DCM and the solution was added dropwise to the reaction mixture. This reaction mixture was allowed to react under the ice-water bath condition for 30 min and then at room temperature for 24 h. After removing insoluble *N,N'*-

dicyclohexylurea (DCU) by suction filtration, an additional 100 mL of distilled water was added to the filtrate and then it was extracted 4 times with 120 mL of DCM. The organic layer was further washed with $NaHCO_3$ and brine solution and dried over anhydrous Na_2SO_4. The solvent was removed by rotary evaporation. It was further purified by silica gel column chromatography using hexane/ethyl acetate as the mobile phase (19: 1 v/v) to get a yellow liquid PDSMA, with a yield of 80%. ^{1}H NMR (Figure S2, DMSO-d_6, δ, ppm): 8.41 (m, 1H, aromatic proton ortho-N), 7.80 (m, 1H, aromatic proton meta-N), 7.77 (m, 1H, aromatic proton para-N), 7.23 (m, 1H, aromatic proton, ortho-disulfide linkage), 6.01 and 5.66 (C=C$\boldsymbol{H}_2$, 2H, s), 4.32 (t, 2H, -C$\boldsymbol{H}_2$OCO-), 3.15 (t, 2H, -S-S-C$\boldsymbol{H}_2$-), 1.83 (C=CC$\boldsymbol{H}_3$, 3H, s). Furthermore, the structure of PDSMA was confirmed by electrospray ionization mass spectrometry (ESI-MS) with observed molecular mass $[M + Na]^+ = 278.76$ *m*/*z* (Figure S3), which matches nicely with the theoretical $[M + Na]^+ = 278.34$ *m*/*z*.

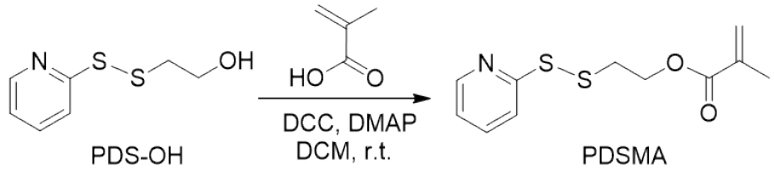

Scheme S2. Synthesis of PDSMA.

Synthesis of pyrene-based CTA. The pyrene–CDP was synthesized following the previously established procedure [4].

Synthesis of a biotin-functionalized PEG-methacrylate (Bt-PEGMA). A dispersion consisting of biotin (1.0 g, 4.1 mmol), HO-PEGMA (2.04 g, 4.1 mmol), EDC (0.86 g, 4.5 mmol), a catalytic amount of DMAP (0.1 g, 0.8 mmol), and DMF (50 mL) was stirred at room temperature for 12 h (Scheme S3) [5]. After 12h, the white precipitate was removed by vacuum filtration, and the solution was evaporated by rotary evaporation. Next, the crude product was re-dissolved and washed with a 5% aqueous $NaHCO_3$ solution and a 1% aqueous HCl solution (2 times each). Solvents were removed by rotary evaporation and the residue was further dried

in a vacuum oven at 45 °C. Finally, the product was collected as a yellow liquid with a yield of 33%. The successful synthesis of the monomer was confirmed by ^{1}H NMR spectra (Figure S4).

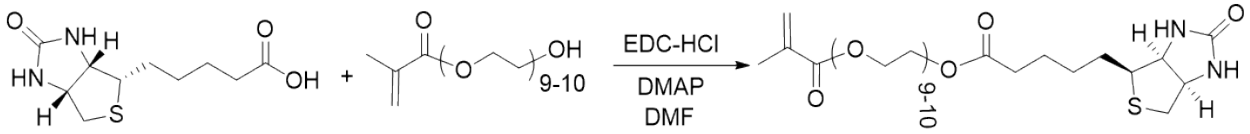

Scheme S3. Synthesis of biotin-functionalized PEG-methacrylate (Bt-PEGMA).

Synthesis of a biotin-functionalized copolymer. The biotin-functionalized polymers were synthesized following a three-step procedure as discussed below.

a) RAFT polymerization of PDSMA and PEGMA. Copolymerization of PDSMA and PEGMA were carried out in DMF at 70 ^{O}C by using pyrene-CDP as the RAFT agent and AIBN as the radical source (Scheme S4). PDSMA (137.76 mg, 0.53 mmol), PEGMA (1.86 g, 6.20 mmol), AIBN (4.42 mg, 2.6×10^{-2} mmol), pyrene-CDP (83.36 mg, 0.13 mmol) and DMF (8.0 g) were placed in a 20 mL reaction vial equipped with a magnetic stir bar. The vial was purged with dry N_2 for 20 min and placed in a preheated reaction block at 70 ^{O}C. After 8 h, the polymerization reaction was stopped by cooling the vial in an ice-water bath and exposed to air. The reaction mixture was diluted with acetone and precipitated into cold hexanes. Then, the polymer was reprecipitated four times from acetone/hexanes and dried under high vacuum at room temperature for 6 h to a constant weight. The purified polymer, **CP1** was isolated as a yellow solid with a yield of 91%. Co-monomer compositions were altered and several copolymers were prepared at [monomer]: [CTA]: [AIBN] = 50: 1: 0.2 ratio. The characterization results for these copolymerization reactions are presented in Table S1.

b) RAFT copolymerization of Bt-PEGMA with CP1 and CP2 as CTA. Copolymerizations of Bt-PEGMA were carried out in DMF at 70 ^{O}C by using **CP1** and **CP2** as the RAFT agent and AIBN as the radical source (Scheme S4). A representative example is as follows: Bt-

PEGMA (440 mg, 0.61 mmol), AIBN (3.97 mg, 2.4×10^{-2} mmol), **CP1** (1.82 g, 0.12 mmol) and DMF (8.0 g) were placed in a 20 mL reaction vial equipped with a magnetic stir bar. The vial was purged with dry N_2 for 20 min and placed in a preheated reaction block at 70 ^{O}C. After 6 h, the polymerization reaction was quenched by cooling the vial in an ice-water bath and exposed to air. The reaction mixture was diluted with acetone and precipitated into cold hexanes. Then, the polymer was reprecipitated four times form acetone/hexanes and dried under high vacuum at room temperature for 6 h to a constant weight. The purified polymer, P((PDSMA-*co*-PEGMA)-*co*-(Bt-PEGMA)), P(**CP1**-*co*-Bt-PEGMA), **CP3** was isolated as a yellow liquid.

2. *In silico* molecular docking study

Computational modeling of CPT1 structure determination, validation and molecular docking with monomer conjugated CoA-SH

Intracellular CPT1A binding potential of **CP4** was predicted through *in silico* molecular docking and Ramachandran plot analysis. Briefly, the 3D structure prediction of CPT1 protein was performed using I-TASSER (Iterative Threading ASSEmbly Refinement) web application tool [6, 7]. For the input amino acid sequence used in I-TASSER tool, sequences of CPT1 were retrieved from UniProt database (UniProtKB - P50416) [8]. Further, using Very 3D (available at https://saves.mbi.ucla.edu/) stereochemical quality of modeled protein was checked and validated. Upon successful validation of the predicted CPT1 modeled structure was further subjected for structure optimization using UCSF Chimera tool (version 1.11.2) [9]. For molecular docking purposes, the modeled crystal structure of CPT1 protein was preprocessed utilizing the 'Protein Preparation Wizard' module [10] of Schrödinger suite. Following the standard protocol of protein preparation [11], the crystal structure of CPT1 was preprocessed. 'Receptor Grid Generation' module used for docking grid file generation embedded in Schrödinger's Maestro interface. Close-proximity amino acid residues along the catalytic

tunnel of CPT1 were selected for grid confinement within the rectangular grid box [12]. Moreover, the X, Y and Z coordinates for the grid center were consigned as 66.0, 16.0, -6.0 Å, respectively. Following the standard protocol of 'LigPrep' [13] module of Schrödinger's suite, energetically optimized 3D low-energy stereoisomers of the monomer conjugated CoA-SH was prepared. The 'Ligand docking' module was used for execution of Glide-XP docking of CPT1 and monomer conjugated CoA-SH [14, 15], following default settings. Only the output parameter was changed as permitting maximum of 6 docked poses per ligand, in result file. Successfully generated docked poses were critically inspected for binding energy using 'XP visualizer' of Schrödinger suite and intermolecular interactions analysis employing protein–ligand interaction profiler (PLIP) [16] application tool.

Molecular dynamics simulation

An all-atomistic molecular dynamics (MD) simulation was performed on the monomer conjugated CoA-SH - CPT1 complex to evaluate the binding interactions stability in a dynamic environment. Therefore, time span of 50 ns MD simulation was carried out using Groningen Machine for Chemical Simulation (http://www.gromacs.org/) tool. Using the Chemistry at Harvard Macromolecular Mechanics 36 (CHARMM36) force field the CPT1 complex topology was generated. The monomer conjugated CoA-SH topology and parameter files were created using SwissParam [17]. The entire complex system was solvated in a cubic box of TIP3P (three-site transferrable intermolecular potential) water molecules confined to 10 Å from the surface of the center of the protein. To neutralize the system, appropriate numbers of ions (Na^+ and Cl^-) were adjusted such as the entire system was maintained at zero. Following a sequential minimization protocol, particularly employing the steepest descent algorithm of 10,000 steps under NVT ensemble, system was substantially equilibrated. The Periodic Boundary Conditions (PBC) was applied in all the axes. The Berendsen thermostat temperature at 300K and Parrinello-Rahman algorithm at 1 bar pressure, all atomistic simulation production

was executed for the prepared complex system under NPT (number of particles (N), pressure (P) and temperature (T)) ensembles for 50 ns production run with a time step of 2 fs to record the simulation events.

3. *In vitro* anticancer assessment

Cell lines

Mice breast cancer cell line, 4T1 and human breast cancer cell lines i.e., MDA-MB-231, MDA-MB-468, normal breast epithelial cell line, MCF-12F were procured from National Centre for Cell Science (NCCS), Pune, Maharashtra, India. All the cell line were revived according to supplier protocol and cultured in Dulbecco modified Eagles media (DMEM) with 10% fetal bovine serum (FBS, Himedia, India), 100 I.U./ml penicillin, 100 µg/ml streptomycin, prior to incubation at 37 °C with 5% CO2 and 95% air until they become confluent. MCF-12F were further supplemented with 10 µg/ml insulin, 0.5 µg/ml hydrocortisone and 20 ng/ml of recombinant EGF supplied by Himedia, India.

Cytotoxicity assay

MTT or 3-(4,5-dimethylthiazol-2-yl)-2,5-diphenyl tetrazolium bromide assay investigated the minimal cytotoxic dose (IC50) of **CP4** in MDA-MB-231, MDA-MB-468, MCF-12F and 4T1 with varying the different concentrations of **CP4** (0, 10, 20, 30, 40, 50, 60, 70, 80, 90 100, 125 µg/ml respectively). From all the cell line, 1×10^4 cells were separately grown in 96 well plate and treated with different concentrations of **CP4** respectively at 37 °C with 24 h of incubation followed by washing with 1X phosphate buffer saline (PBS) and incubation with MTT solutions (1 mg/ml stock) for 4 h at 37 °C. Then, MTT solubilizing buffer solubilized resulting formazan crystal prior to record the individual relative absorbance at 570 nm using microplate reader (BioTek, USA) in triplicate mode.

ROS measurements

CP3 and **CP4**-triggered reactive oxygen species (ROS) generation were investigated by DCFDA method. A green fluorescence of dichlorofluorescein (DCF) indicates the ROS generation after successive interaction of DCF-DA dye with ROS. Based on IC50 dose, untreated control and selective CP4 treated MDA-MB-231 cells were washed with ice-cold PBS and incubated with DCF-DA dye (stock 10 μM) for 30 min at 37 °C and resuspended in PBS to record the data using Flow cytometry (BD Biosciences, Franklin Lakes, NJ, USA) with excitation at 492 and emission at 517 nm. The dye, DCFDA was purchased from HiMedia, India. A comparative ROS analysis was conducted for **CP3** and **CP4** to further validate the selection of **CP4** over **CP3**.

Mitochondrial Membrane potential analysis and morphology analysis

Mitochondrial membrane potential (ΔΨm) determined the cellular function of mitochondria and repolarized state mainly indicates the active function of mitochondria while depolarized state or potential loss indicate inactive function. Intracellular ΔΨm were investigated using JC-1, a cationic dye resulting in the potential dependent changes of fluorescence shift red to green exhibiting mitochondrial depolarization or potential loss. **CP4** treated and untreated MDA-MB-231 cells were incubated with JC-1 dye (stock 10 μg/ml) for 30-40 min at 37 °C after 1X PBS wash and resuspended in PBS prior to record the data using Flow cytometry (BD Biosciences, Franklin Lakes, NJ, USA). The potential transition to monomeric green (529 nm) from aggregate red (590 nm) was applied to investigate the mitochondrial membrane potential. The JC1 dye was procured from Invitrogen, USA. Mitochondrial depolarization was affirmed through the decreased ratio of red/green fluorescence intensities.

Mitochondrial morphology analyses were performed using FESEM analysis after isolation of cellular mitochondria from **CP4** treated or mock-treated breast cancer cells following standard protocol. Briefly, treated or mock-treated cells were individually taken in mitochondria

isolation buffer (MIB) consisting of 640 mM sucrose, 40 mM Tris (pH 7.2) and 2 mM EDTA and centrifuged at 720 g for 10 min. Then, the supernatants were collected and discarded the nuclear pellet. Next, supernatants were further centrifuged at 10000 g for 40 min to collect the mitochondrial pellet. The pellet was then fixed with 2.5% glutaraldehyde for 48 h. After the fixation, the mitochondrial pellet was washed repeatedly and dehydrated by sequential ethanol wash (50, 70, 80, 90, 100 %). Finally, the pellets were immersed in isoamyl alcohol and kept at 4 °C. To perform the FESEM, a monolayer of individual pellet was prepared on a cover slip and dried in vacuum before platinum coating to perform FESEM analysis for mitochondrial morphology investigation.

Mito and Glyco-stress stress analysis

Mito stress associated overall oxygen consumption rate (OCR) and Glyco-stress associates extracellular acidification rate (ECAR) in MDA-MB-231 cells were checked using Seahorse XFe24 Extracellular Flux Analyzer (Seahorse Bioscience, North Billerica, MA, USA) in 24 XFe well plates. For Mito stress analysis, 2×10^4 cells were seeded in XFe24 cell culture plate for 24 h of incubation with 5% CO2 at 37 °C before mock or **CP4**-treatment for 12 h of incubation. Then the post-treatment of cells was washed and replaced with XF base media (Seahorse Bioscience) supplemented with glucose and glutamine for 20-30 min of incubation at 37 °C in a non-CO2 incubator. Next, mitochondria agitating agents, i.e., oligomycin, carbonyl cyanide-4-(trifluoromethoxy)-phenylhydrazone (FCCP) and rotenone/antimycin-A were injected at the drug injection port respectively for basal measurements of OCR with 20 min of calibration and equilibration in the instrument. Following this, the final data were recorded with normalized respective protein content measured by Lowry methods.

Likewise, for ECAR measurement, untreated or **CP4**-treated MDA-MB-231 cells were washed and replaced with XF base media for 1h of incubation at 37 °C in a non-CO2 incubator, supplemented with glutamine. Glucose, oligomycin and 2-deoxyglucose were used as

glycolysis agitating agents at the drug injection ports for 20 min to calibrate and equilibrate the instrument for basal measurements of ECAR. Finally, the data were recoded after normalization with respective protein content measured by Lowry methods. All the mitochondria and glycolysis agitating agents were purchased from Sigma Aldrich.

BODIPY 493/503 staining

To check the lipid uptake fate in presence of **CP4**, 1×10^4 of MDA-MB-231 cells were seeded and incubated overnight at 37 °C and 5% CO_2 incubator prior to **CP4**, P-BSA and mock treatment. Post-treated cells were washed with 1X PBS and fixed in 3.7% paraformaldehyde solution followed by BODIPY (1 mg/ml stock) and DAPI staining in room temperature for 30 min. Finally, the images were captured using Olympus Fluoview confocal laser scanning microscope (Shinjuku, Tokyo, Japan). The excitation/emission wavelength of dye was 503/512 nm.

***In vitro* fatty acid uptake, RNA extraction, cDNA synthesis and gene expression analysis**

RNA was isolated from mock or **CP4-**treated MDA-MB-231 cells following the Trizol method using Trizol reagents supplied by Sigma Aldrich and then transformed the total RNA into cDNA through normal polymerase chain reaction (PCR, Bio-Rad, Hercules, CA, USA) using standard protocols. The relative changes in respective gene expression were performed selecting individual gene-specific forward and reverse primer for CD36 [CD36: *forward 5'-3',* GGATGTCAATGGCTGTCAGGCGTCAG and *reverse 5'-3',* GAGCAGCTGAGAATTCTGGGAGGAGGC], fatty acid synthase [FASN: forward 5'-3', TCGTGGGCTACAGCATGGT and reverse 5'-3', GCCCTCTGAAGTCGAAGAAGAA.], Acetyl-CoA carboxylase α [ACCα: *forward 5'-3', CTGTAGAAACCCGGACAGTAGAAC* and *reverse 5'-3', GGTCAGCATACATCTCCATGTG*], carnitine palmitoyltransferase I [CPT1A: *forward 5'-3', TCCAGTTGGCTTATCGTGGTG* and *reverse 5'-3', CTAACGAGGGGTCGATCTTGG*], ATP citrate lyase [ACLY: *forward 5'-3',*

TGCTCGATTATGCACTGGAAGT and *reverse 5'-3', ATGAACCCCATACTCCTTCCCAG*] and house-keeping gene [β actin: *forward 5'-3', ATGTTTGAGACCTTCAACAC* and *reverse 5'-3', CACGTCACACTTCATGATGG*] by real-time reverse transcriptase-polymerase chain reaction or qPCR (Applied Biosystems, Waltham, MA,USA) using SYBR green (Thermo Fischer Scientific, USA). The calculation of respective gene expression was performed using ΔΔCT or the comparative CT method. Calculation of ΔCT values of the target gene were recorded deducing the ΔCT values of housekeeping gene whereas the comparative fold changes were estimated using the formula: $2^{-[\Delta CT\ (treated) - \Delta CT\ (calibrated)]}$. All the primers were procured from IDT technologies, Iowa, USA.

Anti-migration and invasion study

Scratch assay or wound-healing assay investigated the anti-migratory effect of **CP4** while Transwell (ECM 555, Millipore) chamber assay checked the anti-invasion activities in MDA-MB-231 cells following supplier's standard protocol. For evaluation of anti-migration assay, 1×10^4 of MDA-MB-231 cells were seeded and incubated in 24 well plates for 24 h at 37 °C and 5% CO_2 incubator to achieve the confluence. Next, a scratch on the center of monolayer was drawn with the head of 10 µl tips and treated with mock or **CP4** treatment for a further 12 h and 24 h of incubation respectively at 37 °C. Next, the wound closure activities were observed under an inverted fluorescence microscope (Olympus, Japan) after a specified time interval.

For the anti-invasion assay, 1×10^4 of MDA-MB-231 cells were seeded in a Transwell chamber keeping the nutrients below another chamber overnight at 37 °C and 5% CO_2 incubator. Non-invaded cells were stained with supplied blue dye and washed sequentially to remove dead cells. Next, the invasive cells in the matrix were observed under an inverted fluorescence microscope (Olympus, Japan) and the corresponding intensities were measured using a microplate reader (Biorad, India).

Metastasis related protein expression by ELISA

Anti-migration and invasion-related proteins, matrix metalloproteinase-2 and 9 (MMP-2 and MMP-9) were investigated using a protein specific Enzyme-Linked Immunosorbent Assay (ELISA) kit (Sigma, Aldrich). Briefly, 2.5×10^4 MDA-MB-231 cells were seeded and incubated in ELISA micro plate for 24 h at 37 °C prior to treatment of different concentrations of **CP4** and mock treatment for further 24 h of incubation at 37 °C. Next, all post-treated cells were washed with 1X wash buffer followed by further 20 min of incubation with 1X quenching buffer and replacement with blocking buffer for 1 h of incubation at 37 °C. Next, the cells were washed repeatedly and incubated with 50 µl of 1X primary antibody respectively for 2-3 h of incubation at 37 °C. Then, primary antibody-treated cells were further incubated with 1X HRP conjugated secondary antibody for 1 h at 37 °C after repeated wash with 1X wash buffer followed by the treatment of 100 µl of TMB substrate for 30 min in the dark at room temperature. Finally, the intensities were recorded at 450 nm using microplate reader (BioTek, USA) immediately after the addition of 50 µl of stop solution.

Cell cycle analysis

Cell cycle analyses were performed using the propidium iodide (PI) staining method. Briefly, post harvested cells with **CP4** or mock treatment were incubated for 24 h at 37 °C in 5% CO_2 incubator. Post-treated cells were washed with 1X PBS and stained with PI (25 mg/ml) for 15 min followed by resuspension in PBS. Finally, the data were recorded by Flow Cytometry (BD Biosciences, Franklin Lakes, NJ, USA) with excitation and emission at 493 nm and 636 nm respectively. PI were procured from Invitrogen (Thermo Fisher Scientific, USA).

Apoptosis measurements

Annexin V-FITC staining method checked the programmed cell death or apoptosis. Briefly, **CP4** or mock treated-cells were washed with PBS and resuspended in 100 µl of annexin binding buffer prior to incubation with 5 µl of FITC conjugated Annexin-V (2 µg/ml) followed by the addition of 5 µl of PI (25 mg/ml) for 15 min. Next, the data were recorded using Flow

Cytometry (BD Biosciences, Franklin Lakes, NJ, USA). FITC-conjugated Annexin and PI were procured from Invitrogen (Thermo Fisher Scientific, USA).

4. In vivo anticancer assessment

Animal experiment

The study utilized female nulliparous BALB/c mice (6-7 weeks old, weighing 20-30g) at RG Kar Medical College in Kolkata, India. It was conducted in compliance with the approved protocol by the institutional ethical committee (Approval No. RKC/IAEC/A/03, dated 14/12/2017) and followed the NIH guidelines for laboratory animal maintenance and experimentation [18].

Single-dose toxicity

Acute oral toxicity of **CP4** in mice was tested following the guidelines of OECD No. 423. Briefly, 16 h fasted mice were injected by intravenous route with 1 mg, 5 mg, 10 mg, 15 mg, 20 mg, 30 mg and 40 mg per kg in progressive manner respectively with volume restriction to 0.1 ml/kg for each mouse and observed for 3 days. The behavioral signs and symptoms were carefully noted and recorded. The selection of 50% lethal dose of test formulation was measured by the rate of mortality (if any) up to 14 days.

Selection of therapeutic dosages

Two intravenous dosages i.e., 20 mg/kg and 40 mg/kg (1/5th and 2/5th of maximum studied dose) of **CP4** (**CP4**-20 and **CP4**-40) were selected for therapeutic application in mice based on single-dose acute toxicity whereas 30 mg/kg of Etomoxir (ETO-30) was used as reference anti-tumor drug intravenously every 3 alternative days with volume restriction to 0.1 ml/kg for each mouse.

Tumor induction and assessment

Over-night fasted female BALB/c mice were anesthetized and a 25µl of 4T1 cell suspension of $5x10^4$ cells were injected subcutaneously in the mammary fat pad by 25-gauge needle. After 10 days, all tumor-bearing mice were segregated randomly into four experimental groups (each group containing 6 mice). Then, each group was treated with 20 and 40 mg/kg of **CP4** (**CP4**-

20 and **CP4**-40), 30 mg/kg of Etomoxir (ETO-30) and an equal volume of PBS (0.1 ml/mice) as control intraperitoneal dose with 3 days interval and continued up to 21 days. A time-dependent tumor growth along with mice body weight, tumor weight and volume were calculated and recorded in comparison to tumor control. Tumor volume (V) were measured using caliper and hemi ellipsoid nature of tumor volume were calculated by the formula ½ ×LWH, where LWH denotes mean length, width, and height respectively.

Immunohistochemistry

Post treated mice were sacrificed and tissue were dissected out from individual mice group prior to further processing for tissue histochemistry following paraffin embedding. Tissue-Tek OCT compound embedded tumor and liver tissue were embedded and snap frozen in liquid nitrogen prior to cut into 8 µm thick frozen sections using a cryostat. Then sections were further processed for tissue histochemistry with hematoxylin-eosin (H/E; abcam, USA) staining followed by immunohistochemistry analysis using CPT1A, Ki67, Cleaved caspase 3 antibody (Thermo fisher Scientific, USA) followed by standard protocol.

Tissue biochemistry

Small portion of breast tumor tissue from individual treatment groups were homogenized and taken in phosphate buffer prior to investigate tumor tissue biochemistry. Briefly, homogenized part of breast tissue in 0.1 M phosphate buffer (10% w/v) was prepared to investigate the major oxidative stress parameters including lipid peroxide (LPO), superoxide dismutase (SOD), and reduced glutathione (GSH) following standard protocol. In addition, total cholesterol, high-density lipoprotein (HDL), low-density lipoprotein (LDL), very low-density lipoprotein (VLDL) and triglyceride were also checked spectrophotometrically following standard protocols. To check the nontoxic effect, the live enzymes namely serum glutamate oxaloacetate transaminase (SGOT), serum glutamate pyruvate transaminase (SGPT), alkaline phosphatase

(ALP) and renal markers namely urea, creatinine level were investigated spectrophotometrically using commercially available kits (Arkray, Inc., India).

Statistical Analysis

The experimental data were presented as mean ± s.e.m (standard error of mean) and SD (standard deviation). The levels of significance were calculated using GraphPad Prism version 9.1.0 (221). The significance level was determined using unpaired 2-tailed student t-test, statistical significance considered at $p<0.05$, $p<0.001$, $p<0.001$, and $p<0.0001$.

5. Supplementary Tables

Table S1. Experimental results from the RAFT copolymerization of PDSMA and PEGMA.

Polymer[a]	**PDSMA content in feed**	**Conv.[b] (%)**	**PDSMA content in copolymer[c]**	**$M_{n,theo}$[d] (g mol^{-1})**	**$M_{n,GPC}$[e] (g mol^{-1})**	**$Đ$[e]**	**$M_{n,NMR}$[c] (g mol^{-1})**
CP1	8	91	3	14,100	9900	1.07	15,000
CP2	12	92	4	14,170	10300	1.08	16,000

[a]CP means copolymer. [b]Determined by gravimetric analysis based on the amount of monomer feed. [c]Determined from ^{1}H NMR analysis. [d]$M_{n,theo}$ = (([monomer]/[CTA] × average molecular weight (MW) of monomer × conversion) + (MW of CTA)). [e]Measured by SEC in DMF.

Table S2: Acute toxicity: clinical signs and mortality score in mice

	Group	Incidence of clinical signs observed after dosing at																		Mortality
		Day 1						Day												
		Min.		Hr.																
		10	30	1	2	4	6	2	3	4	5	6	7	8	9	10	11	12	13	14	Total*
Mortality	**CP4**	0	0	0	0	0	0	0	0	0	0	0	0	0	0	0	0	0	0	0	0/3
No Clinical Signs	**CP4**	3	3	3	3	3	3	3	3	3	3	3	3	3	3	3	3	3	3	3	

*Number of mice died/ number of mice treated; N=3 in each group

6. Supplementary figures

Fig. S1-S2

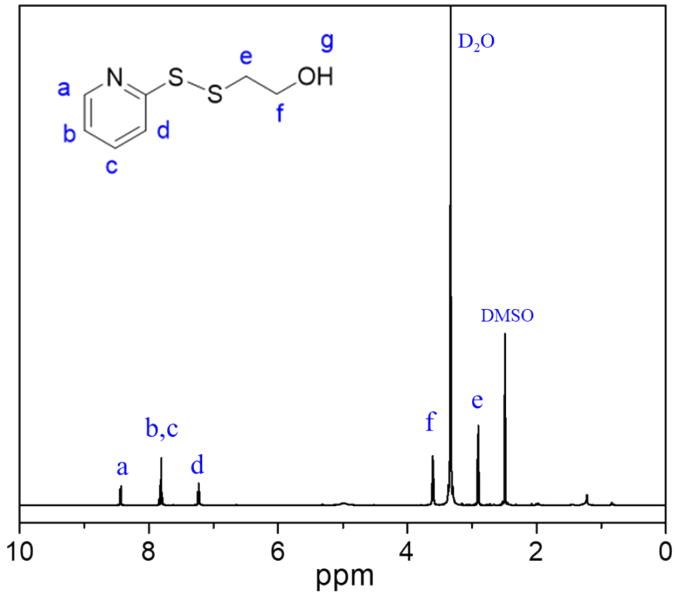

Figure S1. ^{1}H NMR spectrum of PDS-OH in DMSO-d_6.

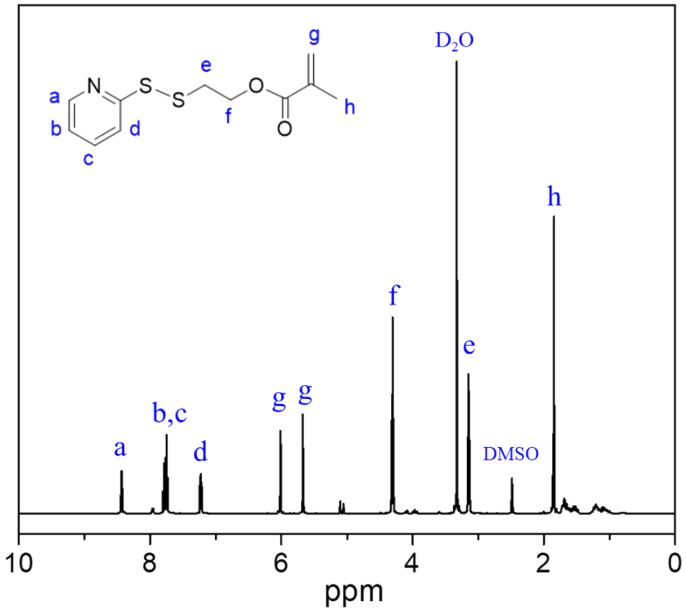

Figure S2. ^{1}H NMR spectrum of PDSMA in DMSO-d_6.

Fig. S3-S4

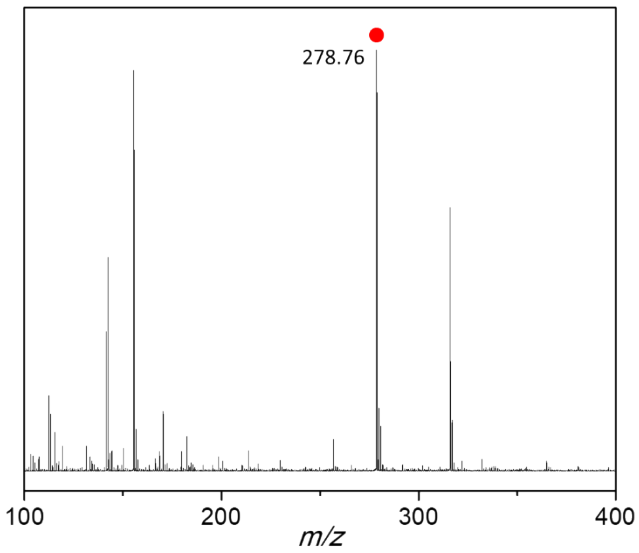

Figure S3. The ESI-MS spectrum of PDSMA.

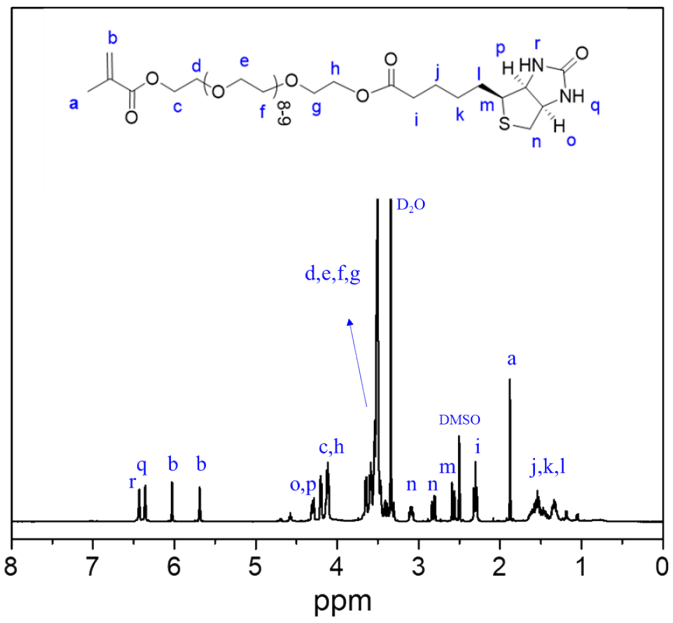

Figure S4. ^{1}H NMR spectrum of Bt-PEGMA in DMSO-d_6.

Fig. S5-S6

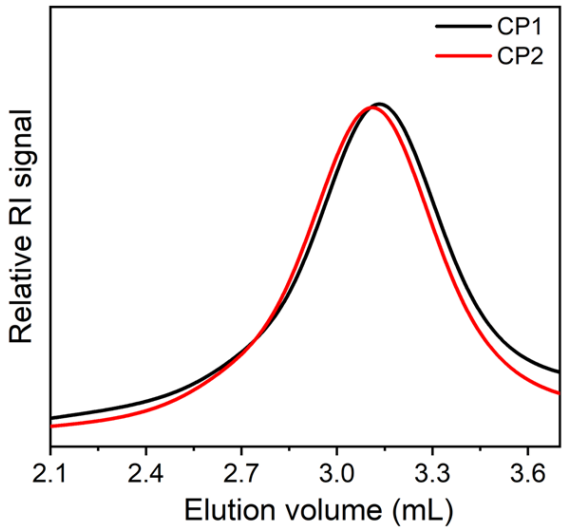

Figure S5. SEC RI traces of P(PDSMA-*co*-PEGMA) (**CP1** and **CP2**) copolymers at different ratios.

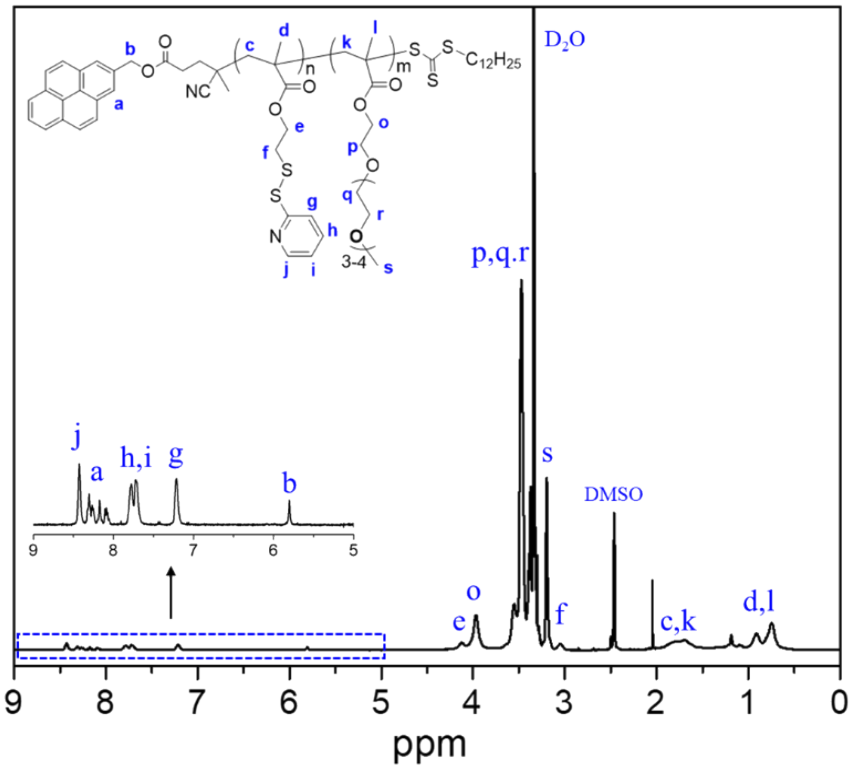

Figure S6. ^{1}H NMR spectrum of **CP1** in DMSO-d_6.

Fig. S7-S8

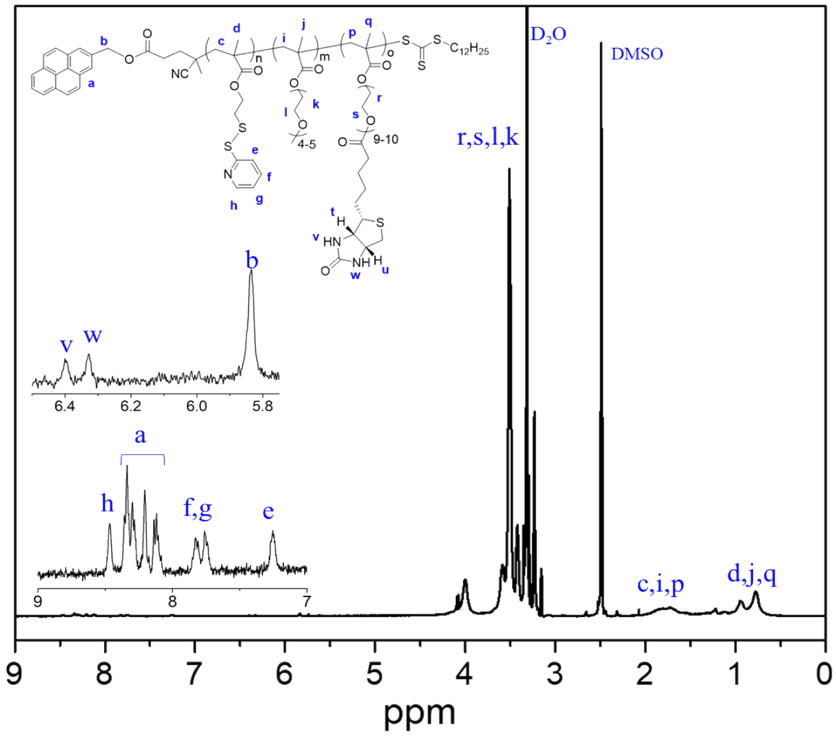

Figure S7. ^{1}H NMR spectrum of P(**CP2**-*co*-Bt-PEGMA), **CP4** in DMSO-d_6.

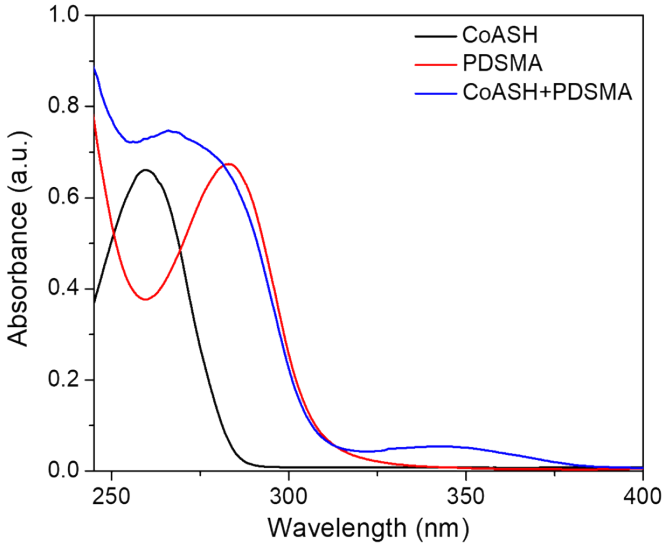

Figure S8. UV-vis spectra of PDSMA (10^{-3} M), CoA-SH (10^{-3} M), and mixture of PDSMA (10^{-3} M) & CoA-SH (10^{-3} M) in tris buffer (H_2O: DMSO = 90: 10 (V/V) at pH 7.5.

Fig. S9.

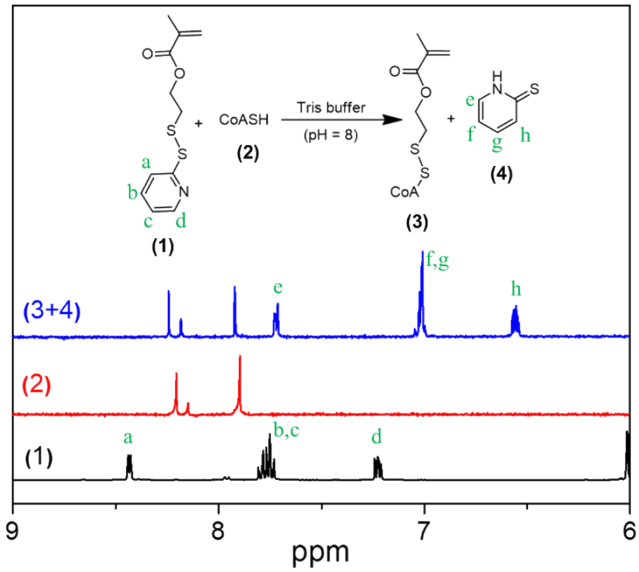

Figure S9. ^{1}H NMR spectra of PDSMA in DMSO-d_6, CoA-SH in D_2O, and both PDSMA & CoA-SH in D_2O-DMSO-d_6 mixture (90: 10 V/V) at pH 7.5.

Fig. S10

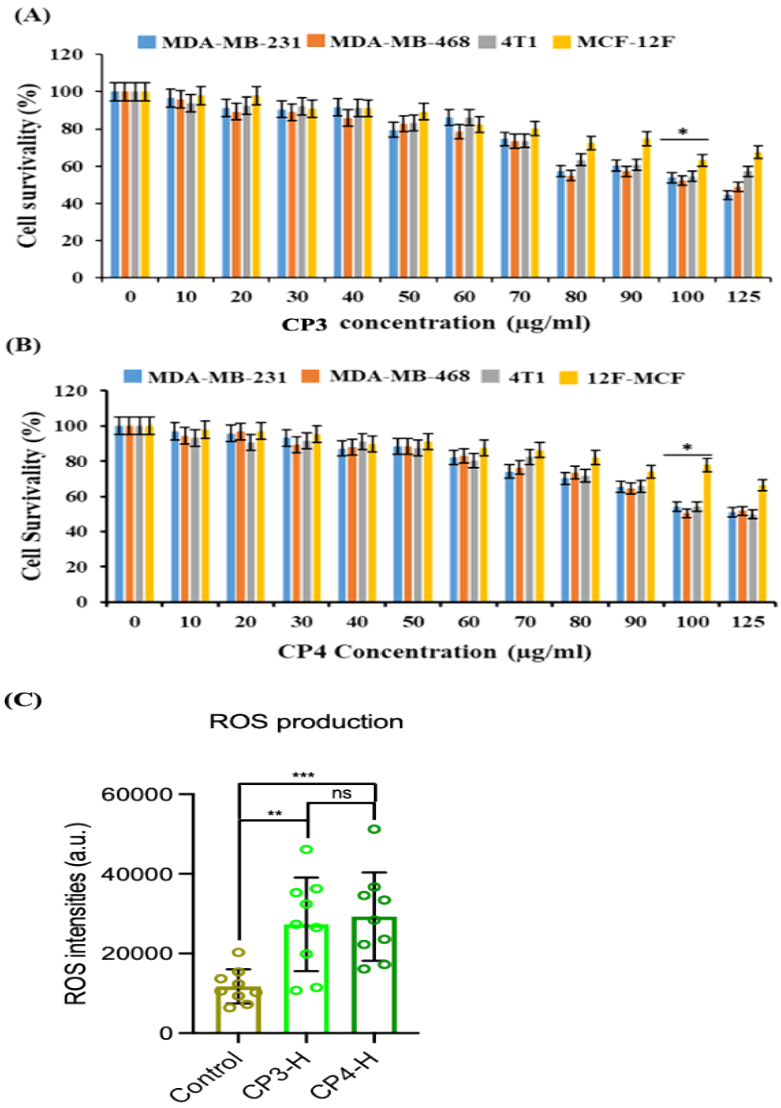

Figure S10. Cytotoxicity assay of **CP3** (A) and **CP4** (B) in different breast cancer cells and compared with untreated control. (**C**) Comparative ROS generation activity of CP3 and CP4 with high dose of 80µg/ml concentrations are depicted and quantified. The level of significance is *$p<0.05$, **$p<0.01$, ***$p<0.001$.

Fig. S11

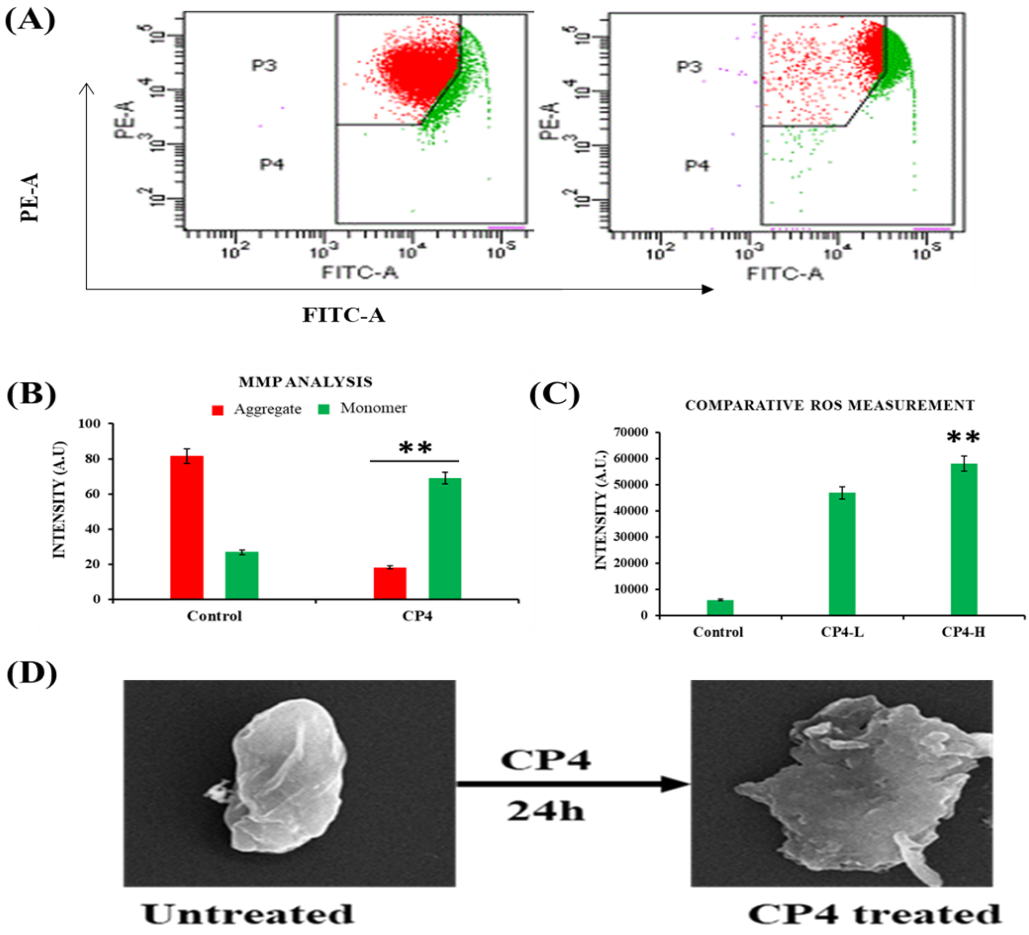

Figure S11. CP4-mediated MMP depletion (A, B) and ROS elevation (C) along with structural deformation of mitochondria (D). The level of significance is ***p<0.01*.

Fig. S12

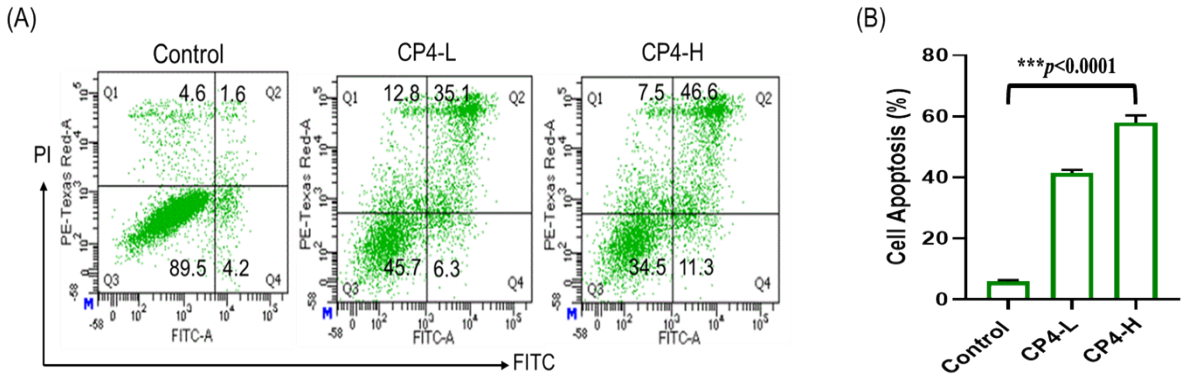

Figure S12. CP4 triggered apoptotic cell death dose-dependently (A). A significant increase in apoptosis is observed in MDA-MB-231 cells treated with CP4 compared to the untreated control, demonstrating a dose-dependent effect (B). Statistical significance is indicated by ****p < 0.001*.

Fig. S13

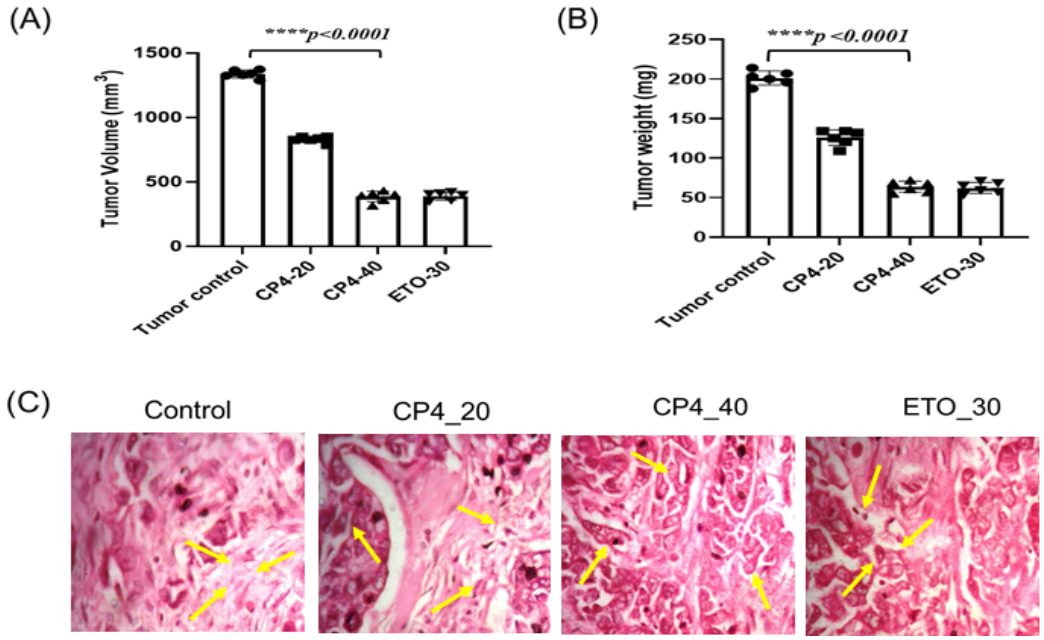

Figure S13. ***In vivo*** **anticancer assessment.** (**A**) **CP4-20, CP4-40,** and **ETO-30** intervened tumor regression has been quantified followed by the tumor weight measurement in figure (**B**) and compared with untreated tumor control. (C) breast tumor tissue histochemistry analysis following H&E staining exhibited necrotic cell lessons. Scale bar 50 μm. The level of significance is ****$p<0.0001$.

Fig. S15

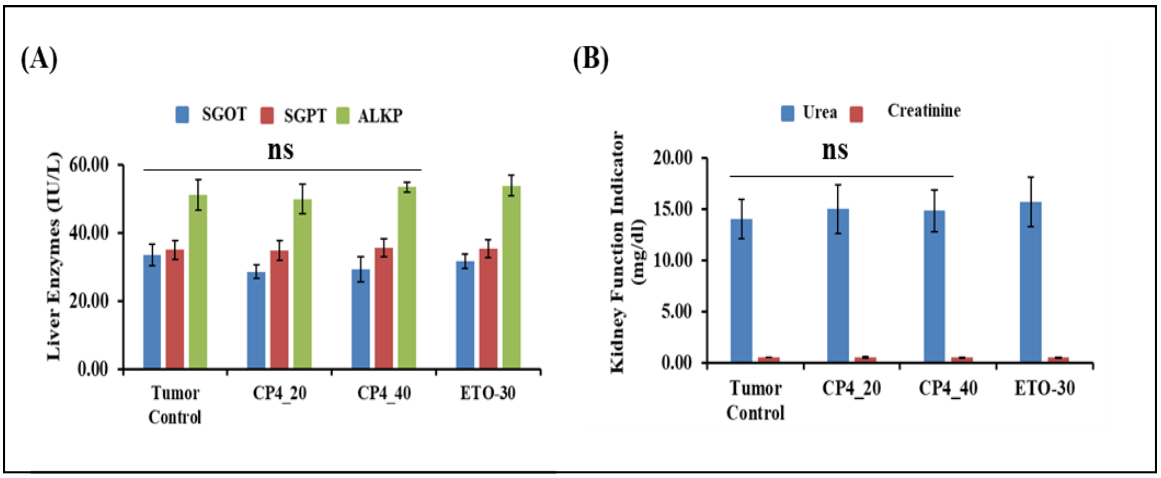

Figure S14. Profiling of kidney and liver enzymes. (A) Non-significant changes in liver enzymes level such as, serum glutamate oxaloacetate transaminase (SGOT), serum glutamate pyruvate transaminase (SGPT), alkaline phosphatase (ALP) and **(B)** kidney function indicator, Urea and Creatinine level. '**ns**' denotes non-significant.

7. References.

[1] Moad G, Chong YK, Postma A, *et al*. Advances in RAFT polymerization: the synthesis of polymers with defined end-groups. *Polymer* 2005; *46*: 8458-8468.

[2] Ghosh S, Basu S, Thayumanavan S. Simultaneous and reversible functionalization of copolymers for biological applications. *Macromolecules* 2006; **39**: 5595-5597.

[3] Kumar S, Roy SG, De P. Cationic methacrylate polymers containing chiral amino acid moieties: controlled synthesis via RAFT polymerization. *Polym. Chem*. 2012; *3*: 1239–1248.

[4] Kumar S, De P. Fluorescent labelled dual-stimuli (pH/thermo) responsive self-assembled side-chain amino acid-based polymers. *Polymer* 2014; *55*: 824-832.

[5] Aleksanian S, Khorsand B, Schmidt R, *et al*. Rapidly thiol-responsive degradable block copolymer nanocarriers with facile bioconjugation. *Polym. Chem.* 2012; *3*: 2138-2147.

[6] Yang J, Yan R, Roy A, *et al*. The I-TASSER Suite: protein structure and function prediction. *Nat. Methods* 2015; *12(1)*: 7-8.

[7] Roy A, Kucukura A, Zhang Y. I-TASSER: a unified platform for automated protein structure and function prediction. *Nat. Protoc.* 2010; *5(4)*: 725-738.

[8] Consortium TU. UniProt: a worldwide hub of protein knowledge. *Nucleic Acids Res.* 2018; *47(D1)*: D506-D515.

[9] Pettersen EF, Goddard TD, Huang CC, *et al*. UCSF Chimera--a visualization system for exploratory research and analysis. *J. Comput. Chem.* 2004; *25(13)*: 1605-1612.

[10] Protein Preparation Wizard; Schrödinger, LLC, New York, NY, **2018**.

[11] Sastry GM, Adzhigirey M, Day T, *et al*. Protein and ligand preparation: parameters, protocols, and influence on virtual screening enrichments. *J. Comput Aided Mol. Des.* 2013; *27(3)*: 221-234.

[12] Lopez-Vinas E, Bentebibel A, Gurunathan C, *et al*. Definition by functional and structural analysis of two malonyl-CoA sites in carnitine palmitoyltransferase 1A. *J. Biol. Chem.* 2007; *282(25)*: 18212-18224.

[13] LigPrep. Schrödinger, LLC, New York, NY, **2018**.

[14] Friesner RA, Banks JL, Murphy RB, *et al*. Glide: A New Approach for Rapid, Accurate Docking and Scoring. 1. Method and Assessment of Docking Accuracy. *J. Med. Chem.* 2004; *47(7)*: 1739-1749.

[15] Friesner RA, Murphy RB, Repasky MP, *et al*. Extra precision glide: docking and scoring incorporating a model of hydrophobic enclosure for protein-ligand complexes. *J. Med. Chem.* 2006; *49(21)*: 6177-6196.

[16] Salentin S, Schreiber S, Haupt VJ, *et al*. PLIP: fully automated protein-ligand interaction profiler. *Nucleic Acids Res* 2015; *43(W1)***:** W443-447.

[17] Zoete V, Cuendet MA, Grosdidier A, *et al*. SwissParam: a fast force field generation tool for small organic molecules. *J. Comput. Chem.* 2011; *32(11)***:** 2359-2368.

[18] Ruidas B, Sur TK, Pal K, *et al*. Herbometallic nano-drug inducing metastatic growth inhibition in breast cancer through intracellular energy depletion. Mol. Biol. Rep. 2020; 47: 3745-3763.